Materials Letters 394 (2025) 138623

Contents lists available at ScienceDirect

Materials Letters

journal homepage: www.elsevier.com/locate/matlet

Cellulose Nanofiber/Chitosan/Polyrotaxane foam alloy for sustainable form-stable phase change materials

Xiao-Mei Yang [a,b,*], Luis Soliverdi Mesa [b], Adolfo Nadal Serrano [b], Guang-Zhong Yin [b,*]

[a] Faculty of Diseño, Innovación y Tecnología, Universidad de Diseño, Innovación y Tecnología (UDIT), Av. Alfonso XIII, 97, 28016 Madrid, Spain
[b] Universidad Francisco de Vitoria, Ctra. Pozuelo-Majadahonda Km 1.800, 28223 Madrid, Spain

ARTICLE INFO

Keywords:
Cellulose nanofiber
Porous materials
Polyrotaxane
PEG

ABSTRACT

This study introduces a novel cellulose nanofiber (CNF)/Chitosan (CH)/polyrotaxane (PLR) foam alloy as a form-stable PCM support material. The CNF/CH/PLR aerogel demonstrates a well-balanced porous structure with effective encapsulation of polyethylene glycol (PEG). Combining PLR with CNF/CH, the PEG leakage resistance was significantly improved. The resulting CNF/CH/20 %PLR-PEG composite exhibits exceptional enthalpy values of 181.1 J/g, along with superior mass retention rates under melting. These findings highlight the potential of this bio-based composite for advanced thermal energy storage systems, offering a sustainable and efficient solution for energy-efficient applications.

1. Introduction

The growing demand for sustainable materials has led to increasing interest in the use of natural polymers for advanced applications. Among these, cellulose nanofibers (CNFs), derived from renewable biomass, have garnered significant attention due to their excellent mechanical properties, biodegradability, and lightweight nature [1]. CNFs are particularly promising for fabricating lightweight porous structures, such as aerogels, which can be applied in various fields, ranging from thermal insulation to energy storage. However, CNF-based aerogels sometimes face challenges with structural uniformity and stability. Their irregular microstructures and poor shape retention limit their use, especially in applications requiring well control of material properties, such as phase change material (PCM) encapsulation for thermal management. Notably, in recognition of their excellent capacity for regulating thermal energy harvesting [2,3], storage and release, PCMs have been rediscovered and received growing significance in advanced energy conversion, harvesting, storage and thermal management [4–7].

To address the challenges of the irregular microstructures and poor shape retention, biopolymers like chitosan (CH) offer a promising solution. CH is known for its biocompatibility and ability to form strong films [8]. Additionally, polyrotaxane (PLR) exhibits excellent leakage resistance, making it highly suitable for encapsulating PEG-based PCMs [9]. By incorporating CH into the CNF matrix, we aim to enhance the microstructural integrity and shape stability of CNF aerogels. The further introduction of PLR, whose main chain is Poly (ethylene oxide) (PEO), can improve compatibility with PEG, enhancing the anti-leakage properties—critical for effective Polyethylene glycol (PEG) encapsulation [10]. This study will focus on how these modifications influence microstructure, shape retention, and the potential of the aerogels as PCM support materials, to provide insights into the design of sustainable and efficient materials for thermal energy storage applications.

2. Experimental

2.1. Materials

CH and PEG (6000 g/mol), PEO (1×10^6 g/mol) and α-cyclodextrin (α-CD, 98 %) were all purchased from Sigma-Aldrich and used as received. CNF suspension (1.75 wt. %) was kindly provided by the University of Oulu.

2.2. CNF/CH aerogel

A CNF suspension was mixed with 3 wt. % CH solution with adjustable ratio (w/w = 8/2; 7/3; 6/4; and 10/0). The CNF/CH mixture was then poured into cylindrical molds, freeze-dried at -50 °C for 48 h to produce the aerogel.

* Corresponding authors.
E-mail addresses: xiaomei.yang@udit.es (X.-M. Yang), amos.guangzhong@ufv.es (G.-Z. Yin).

https://doi.org/10.1016/j.matlet.2025.138623
Received 17 January 2025; Received in revised form 12 March 2025; Accepted 22 April 2025
Available online 23 April 2025

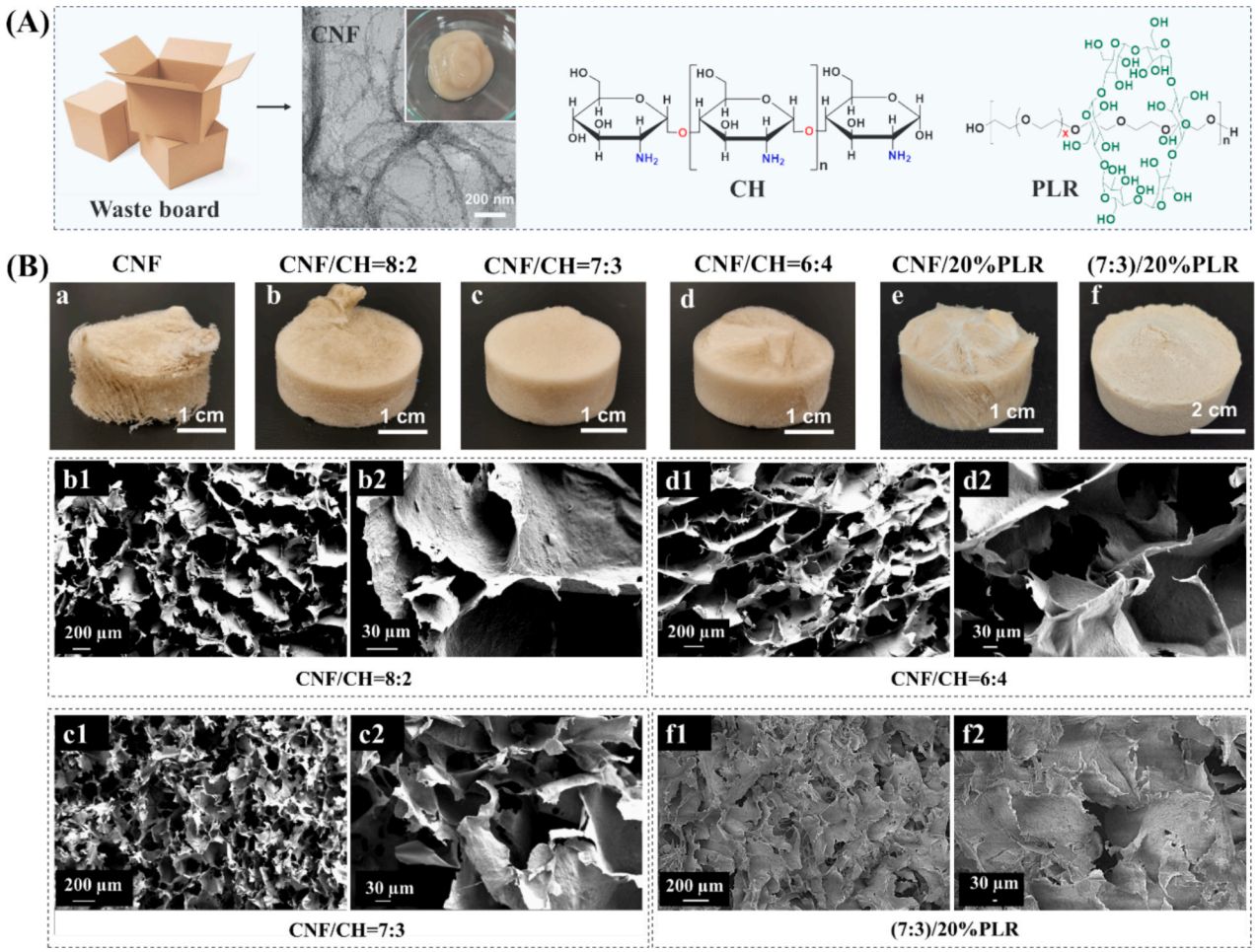

Fig. 1. (A) The raw materials for the fabrication of the sustainable aerogels: CNF, CH and PLR, (B) Image of a set of CNF composites with varying ratios of CH and PLR, accompanied by SEM images.

2.3. Preparation of PLR

PEO (3 g) was dissolved in H_2O (80 mL) at 80 °C, and then α-CD (1.5 g) was slowly added. The reaction mixture was cooled down and kept at 4 °C for 72 h to yield the PLR solution. FTIR (cm^{-1}): 3352, 2875, 1651, 1341, 1278, 1241, 1097, 1027.

2.4. CNF/CH/PLR aerogel

The mixture was obtained by maintaining a weight ratio of 7:3:2 for suspension CNF, CH solution and PLR solution, respectively. The CNF/CH/PLR mixture was then freeze-dried to produce a three-dimensional network. CNF/PLR (7:3) foam was also prepared as a reference sample by the same process.

2.5. Characterizations

Molten PEG was absorbed into the foam at 80°C. The cross-sectional morphology of the aerogels was examined using scanning electron microscopy (SEM). Differential scanning calorimetry (DSC, TA Q25) was employed to detect thermal transitions. Leakage behavior was evaluated by recording the weight changes over time at 80 °C. Mass retention rates were obtained by the following equation: $Mass\ retention\ rate = \frac{m_t}{m_0} \times 100\%$, where m_t is the mass after heating at 80 °C for 3 h and m_0 is the initial mass. Cycle performance was recorded by DSC following the methods described in the literature elsewhere [11,12].

3. Results and discussion

By adjusting the ratio of CNF, CH and PLR, we aim to identify the optimal proportion that yields a well-defined microporous structure. Fig. 1 displays the raw materials and morphology of CNF, along with the structure of CH and PLR (Fig. 1A). It also includes a series of CNF-based aerogels with varying ratios of CNF, CH, and PLR (Fig. 1B), accompanied by corresponding SEM images. The macrostructures (Fig. 1B(a–f)) highlight the impact of different formulations on aerogel morphology. The CNF foam (a) exhibits a loose structure with visible irregularities, reflecting poor structural integrity. The CNF/CH samples (b-d) show significantly improved uniformity, with the CNF/CH (7:3) sample (c) displaying the most uniform structure. The (7:3)/20 % PLR sample (f) also exhibits uniform structure, demonstrating a stable and optimized design.

The SEM images (Fig. 1B: b1-f2) reveal the microstructural differences across the aerogels. The CNF/CH-8:2 sample exhibits a porous structure with unevenly distributed voids, while the CNF/CH-7:3 sample shows a more uniform and compact network with smaller, evenly distributed pores. In contrast, the CNF/CH-6:4 sample presents larger and less defined pores, which may compromise its structural integrity. The (7:3)/20 %PLR sample stands out with well-defined pores. These characteristics make it highly suitable for applications requiring effective PCM containment and reliable leak prevention.

Fig. 2a briefly shows the process of aerogel absorbing PEG and the physical appearance of the samples before and after absorption. Fig. 2b presents the identical chemical structure of the PEG molecular chain and

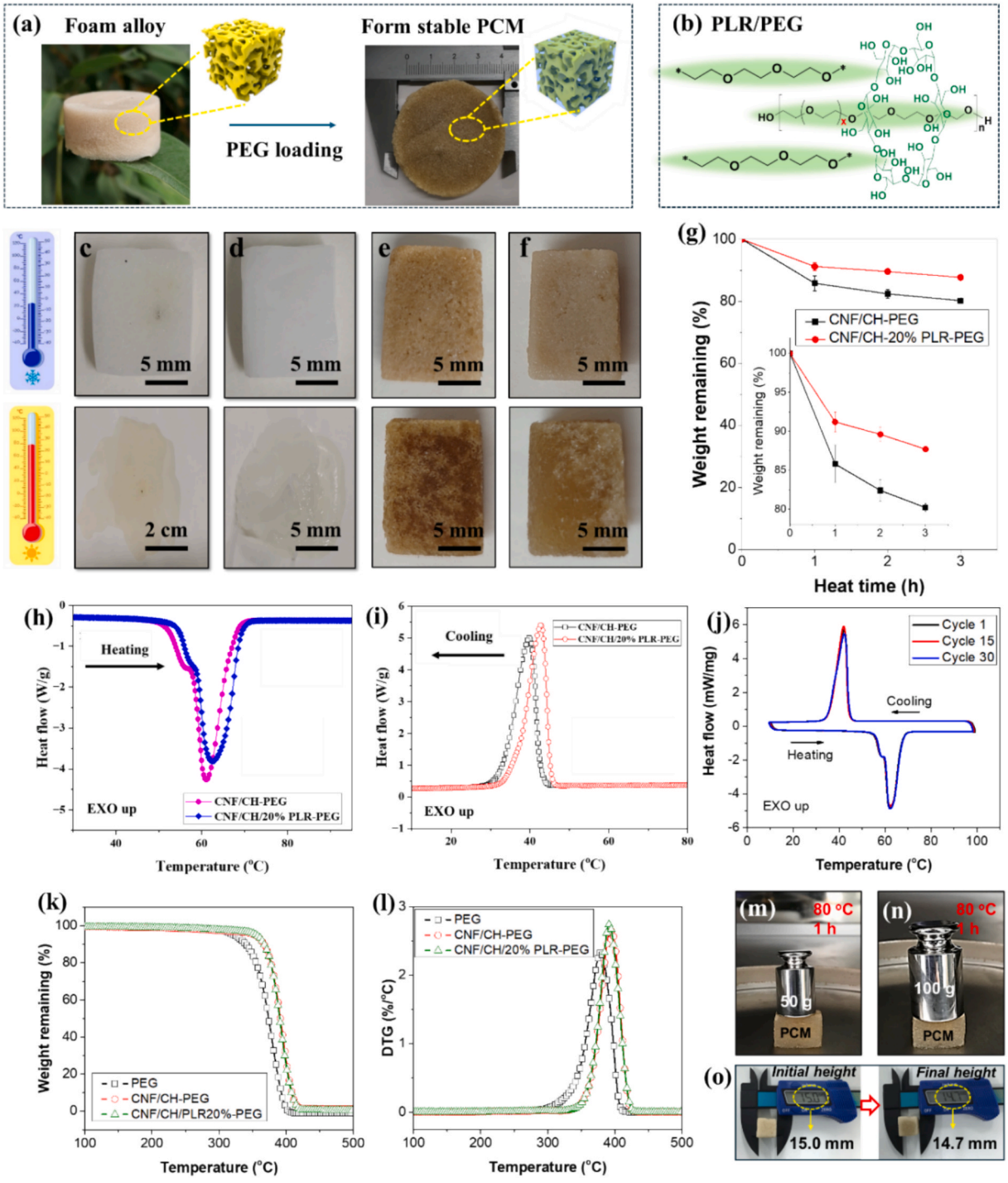

Fig. 2. (a) Encapsulation illustration of the PCMs, (b) main chain of PLR and PEG structure, form stability test: (c) PEG, (d) PLR-PEG, (e) CNF/CH-PEG, and (f) CNF/CH-20 % PLR-PEG before and after heating at 80 °C for 3 h; (g)The leakage curve of the sample CNF/CH/20 % PLR-PEG, DSC heating (h) and cooling curves (i) for CNF/CH-PEG and CNF/CH-20 % PLR-PEG, respectively; (j) cycle test of sample CNF/CH/20 % PLR-PEG, (k) TGA and (l) DTG curves of PEG, CNF/CH-PEG and CNF/CH/20 % PLR-PEG, (m) A 50 g and (n) 100 g weight placed on top of the heated PCM composite sample; and (o) Sample height before and after hot/press treatment.

the PLR main chain. Subsequently, PEG, PLR/ PEG, CNF/CH/20 % PLR-PEG, and CNF/PLR-PEG were selected as representative samples to analyze the shape stability and leakage resistance. Fig. 2(c–f) presents photographs of PEG, PLR-PEG, CNF/CH-PEG, and CNF/CH-20 % PLR-PEG before and after heating. After heating at 80°C for 3 h, PEG completely melted, PLR-PEG exhibited significant deformation collapse. In contrast, CNF/CH-PEG and CNF/CH-20 % PLR-PEG almost maintained their initial shape. Notably, their mass retention rates were 80.2 ± 0.5 % for CNF/CH-PEG and 87.7 ± 0.3 % for CNF/CH-20 % PLR-PEG, highlighting the significant role of PLR in enhancing leakage resistance. Regarding the improvement of PEG leakage resistance in porous materials by PLR, we believe that its main chain can melt at 80 °C and share the same chemical structure as PEG (Fig. 2b), which effectively ensures interfacial compatibility between the support material and PEG. Fig. 2g further shows the leakage curves, visually demonstrating that the sample containing PLR has significantly improved anti-leakage performance.

The DSC graphs in Fig. 2(h, i) illustrate the thermal behavior of CNF/

Table 1
Specific indicators of the selected samples.

Samples	Melting Enthalpy (J/g)	Solidification enthalpy (J/g)	PCM loading (%)	Mass retention rate (%)
CNF/CH-PEG	179.8	174.3	97.94	**80.2 ± 0.5**
CNF/CH/20 %PLR-PEG	181.1	175.9	97.69	**87.7 ± 0.3**

Table 2
Some comparison of latent heat of biobased PCM.

No.	Work substances	Support materials	Enthalpy (J/g)	Ref.
1	PEG1000	Prosopis juliflora biochar	146.7	[16]
3	PEG4000	Sunflower stem carbon	153.4	[17]
6	PEG6000	TEMPO-oxidized CNF	172.1	[18]
7	PEG1000-2000	Pleurotus eryngii carbon	174.9	[19]
8	PEG4000	Porous carbon fiber-MWCNTs	156.6	[20]
9	PEG6000	CNF/CH-20 %PLR	181.1	This work

CH-PEG and CNF/CH-20 % PLR-PEG, emphasizing their high enthalpy values. Typically, CNF/CH-PEG exhibits enthalpy values of 179.82 J/g (heating) and 174.27 J/g (cooling), while CNF/CH-20 % PLR-PEG has slightly increased values to 181.08 J/g and 175.87 J/g, respectively. This may be because, at the same PEG loading (~97 %, Table 1), the PLR component of the supporting framework can also melt, contributing a small amount to the phase change enthalpy. Similar results can be found in our previous report [13].

Fig. 2j shows the cycling curves of the optimized sample (CNF/CH/20 % PLR-PEG), indicating that the sample exhibits good cycling stability. Additionally, we conducted TGA on PEG, CNF/CH-PEG, and CNF/CH/20 % PLR-PEG (Fig. 2k–l). We found that the two form-stable samples exhibit very similar trends (with T_{95} around 350°C), and both are higher than that of PEG (T_{95} ~ 330 °C). This may be due to the spatial barrier effect of the support materials, which delays the release of decomposition components. Inspired by the literatures [14,15], we conducted compressive tests on the optimized sample in the molten state (Fig. 2m–o). We found that the sample exhibited excellent mechanical support even PEG was completely molten.

Table 2 compares various PCMs based on their support materials, and enthalpy values, highlighting our work, PEG with CNF/CH-20 % PLR-PEG, with an exceptional enthalpy value of 181.1 J/g. This performance surpasses high-performing bio-based alternatives such as TEMPO-oxidized CNF (172.1 J/g), and sunflower stem carbon/polyethylene glycol (153.4 J/g). These results position our material as a promising and sustainable solution for advanced energy-efficient applications.

4. Conclusion

A novel CNF/CH/PLR foam alloy was developed as a support material for form-stable PCMs, demonstrating excellent thermal energy storage performance and structural stability. The incorporation of chitosan improved the microstructural integrity of the CNF aerogels, while Polyrotaxane remarkably enhanced leakage resistance and compatibility with PEG-based PCMs. The resulting CNF/CH/20 %PLR-PEG composite achieved outstanding enthalpy values, along with exceptional shape retention and minimal weight loss during thermal cycling. These results establish the CNF/CH/PLR foam alloy as a highly promising, bio-based solution for advanced thermal energy storage systems, addressing key challenges in leakage prevention and sustainability.

CRediT authorship contribution statement

Xiao-Mei Yang: Writing – review & editing, Writing – original draft, Investigation, Formal analysis, Data curation. **Luis Soliverdi Mesa:** Writing – review & editing, Data curation. **Adolfo Nadal Serrano:** Writing – review & editing, Data curation. **Guang-Zhong Yin:** Writing – review & editing, Resources, Project administration, Funding acquisition, Conceptualization.

Declaration of competing interest

The authors declare that they have no known competing financial interests or personal relationships that could have appeared to influence the work reported in this paper.

Acknowledgment

This work was supported by NEWSAFE (No.: PID2022-143324NA-I00) Projects funded by: MICIU (Ministerio de Ciencia, Innovación y Universidades)/AEI (Agencia Estatal de Investigación); and Ramón y Cajal Fellowship (No.: RYC2023-045023-I) funded by: MICIU. This work was also partially supported by INC-UDIT-2025-JCR25 and INC-UDIT-2025-PRO21. The authors are deeply grateful to the Nanostructured Lignocelluloses Research Team in the Fibre and Particle Engineering research unit at the University of Oulu (led by prof. Henrikki Liimatainen) for kindly providing the CNF.

Data availability

No data was used for the research described in the article.

References

[1] D. Klemm, et al., Angew. Chem. Int. Ed. 44 (2005) 3358–3393.
[2] H. Jiang, et al., J Mate Sci Technol 209 (2025) 207–218.
[3] R. Yan, et al., Int J Biol Macromol 277 (2024) 134233.
[4] Y. Huang, et al., ACS Sustainable Chem Eng 12 (2024) 4662–4675.
[5] J. Lin, et al., Small 20 (2024) 2402938.
[6] Y. Cao, et al., Adv. Compos. Hybrid Mater. 8 (2025) 104.
[7] Y. Ma, et al., Sol Energ Mater Sol C 276 (2024) 113078.
[8] M. Rinaudo, Prog. Polym. Sci. 31 (2006) 603–632.
[9] G.-Z. Yin, et al., Chem. Eng. J. 444 (2022) 136421.
[10] S. Chakraborty, et al., J. Storage Mater. 28 (2020) 101275.
[11] Y. Liu, et al., Sep. Purif. Technol. 354 (2025) 129541.
[12] Y. Liu, et al., Desalination 585 (2024) 117783.
[13] G.-Z. Yin, et al., Int J Biol Macromol 222 (2022) 429–437.
[14] Y. Xiao, et al., Sol Energ Mater Sol C 282 (2025) 113369.
[15] X. He, et al., Adv. Funct. Mater. 34 (2024) 2409675.
[16] A. Yadav, et al., Mater. Today Commun. 38 (2024) 108114.
[17] N. Gao, et al., RSC Adv. 14 (2024) 24141–24151.
[18] Y. Pang, et al., Int J Biol Macromol 264 (2024) 130633.
[19] J. Shi, et al., Adv Compos Hybrid Mater 7 (2023) 2.
[20] Y. Jiang, et al., Mater. Lett. 377 (2024) 137385.